Bulletin of the Seismological Society of America, Vol. 106, No. 6, pp. 2831–2842, December 2016, doi: 10.1785/0120150305

Analytical Estimation of Short-Period Ground Motions in Mexico City for Engineering Applications

by Masahiro Iida

Abstract In previous studies, short-period (0.2–5.0 s) ground motions in Mexico City were investigated by a systematic analysis of surface and downhole accelerograms, and it was found that short-period Love waves were very dominant at the predominant periods of grounds. Although the average vertical amplification of ground motions with long duration was interpreted fairly well at soft-soil sites, the large time variations in the vertical amplification remain unexplained. The present study addresses two issues on the vertical amplification at two soft-soil sites, which are important for engineering applications. The first issue is the interpretation of the large time variations in the vertical amplification of ground motions, and the influence of the depth of the structure in which surface waves are trapped is examined. The second issue is the interpretation of inertial force excitation, which is usually used in the engineering community, in terms of seismic waves. The second issue is also estimated by the vertical amplification. The conclusions are as follows: (1) the large time variations in the vertical amplification of ground motions can be explained sufficiently by both the mixture of *S* waves and Love waves and the depth of the structure in which Love waves are trapped. The structure corresponds to the Mexico City basin. (2) Although inertial force excitation is considered to be valid for *S* waves, it proves to be invalid for Love waves.

Introduction

Short-period (less than a few seconds) surface waves play a very important role in the engineering community, which will be clearly demonstrated in the present study. Up until now, short-period surface waves have not received much attention. Certainly, the presence of short-period surface waves observed at a soft-soil site has been pointed out in a variety of studies (e.g., Johnson and Silva, 1981; Kinoshita *et al.*, 1992). However, the significant characteristics of short-period surface waves have not been evaluated quantitatively.

We continue to investigate the nature of short-period ground motions in Mexico City (Iida and Kawase, 2004; Iida, 2007b) and in Tokyo (Iida *et al.*, 2005; Iida, 2007a). The original motivation was that short-period ground motions could not be explained satisfactorily at soft-soil sites in the two metropolitan areas, using conventional approaches such as inertial force excitation used in the engineering community and *S*-wave theoretical amplification. This insufficiency will be evidently shown in the present study. The fundamental cause of unsatisfactory explanation was that short-period surface waves were not taken into account quantitatively, in spite of the distinct presence. Surface waves are included very much in short-period ground motions at soft-soil sites.

Referring to our previous investigations made in Mexico City (Fig. 1), two preliminary studies (Iida, 1999, 2000) showed that short-period surface waves were very dominant in the Valley of Mexico, on the basis of a cross-correlation analysis between surface and downhole recordings. Moreover, two succeeding studies (Iida and Kawase, 2004; Iida, 2007b) explained well the remarkable vertical amplification of ground motions observed at soft-soil sites, by taking into account Love waves trapped in an intermediate-depth (1000 m) structure. Also, in the succeeding studies, by applying an improved version of a stochastic method by Kinoshita (1981, 1999) to surface and downhole recordings, surface recordings were separated into *S*-wave and surface-wave seismograms.

Next, following the above-mentioned estimations of ground motions, a seismic wavefield was constructed for a deep structure by elastic wave theory, and a new nonlinear soil response method based on an input wavefield was proposed (Iida, 2006). An input wavefield means that forces produced by body waves and surface waves propagating in a small soil volume are employed as external forces. The linear soil response was able to reproduce the input wavefield very well. As a natural extension, new soil–building interaction analyses based on an input wavefield were successfully performed in a regular interaction system (Iida, 2013; Iida *et al.*, 2015). Consequently, it was demonstrated that input wavefield excitation was more reasonable than inertial force

excitation on the bottom boundary of the system in soil and building response analyses.

However, throughout the series of studies, two unsolved issues on the vertical amplification of ground motions in surface layers are important for engineering applications. The present study addresses the two issues at two soft-soil sites in Mexico City. Although the average vertical amplification of ground motions with long duration in surface layers was interpreted fairly well at the two soft-soil sites (Iida and Kawase, 2004; Iida, 2007b), the large time variations in the vertical amplification remain unexplained. First, the large time variations in the vertical amplification of ground motions are interpreted.

Second, because inertial force excitation is usually used in the engineering community, the validity is examined in terms of seismic waves. Undoubtedly, inertial force excitation has played a significant role. The excitation has strong points that the treatment is very simple, and the solution obtained by the excitation is always stable. However, the physical basis is not very clear. Hence, it is questionable if inertial force excitation is able to express seismic waves properly. The second issue is also estimated by the vertical amplification. In the present study, the target period range of engineering concern is between 0.2 and 5.0 s. In past cases, as the shallow (several tens of meters) soil profile becomes softer, the analytical estimation of ground motions gets much more difficult. Because Mexico City possesses extremely soft soils, the present study is challenging.

In the present article, first, representative studies for ground motions in Mexico City are reviewed. In the Vertical Amplitude Ratios section, at two soft-soil sites, we make a basic nonstationary analysis of surface and downhole recordings, through amplification estimation and a cross-correlation technique that identifies *S* waves and surface waves. Then, inertial force excitation is examined in terms of *S* waves and surface waves. As surface waves, the fundamental modes of resonance of Love waves and Rayleigh waves are considered. Moreover, the large time variations in the vertical amplification of ground motions are interpreted by means of surface waves. Throughout the present article, while the two horizontal components of recordings are analyzed, the east–west component accelerations are displayed.

Ground Motions in Mexico City

In this section, representative studies for ground motions in Mexico City, which were made after the 1985 Michoacan earthquake, are reviewed, followed by a description of the analytical estimations of ground motions. The 19 September 1985 M_s 8.1 Michoacan earthquake caused extreme damage in the lakebed zone of Mexico City located inside of the Valley of Mexico, which is ~400 km from the epicenter in the Pacific Ocean (e.g., Meli and Avila, 1989). The Valley of Mexico is divided into three geotechnical zones: (1) the hill zone, (2) the transition zone, and (3) the lakebed zone (Fig. 1).

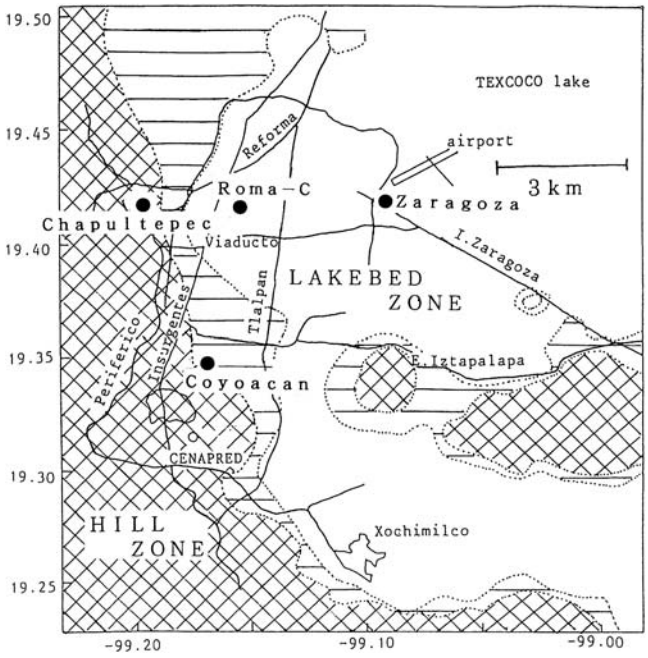

Figure 1. The Valley of Mexico showing the hill, transition, and lakebed zones. The three zones are indicated by the criss-cross, line, and blank patterns, respectively. Although the hill zone occupies the southwestern areas, the lakebed zone extends to the central and northeastern areas. The transition zone is located between these two zones. Four strong-motion borehole stations are indicated by filled circles.

The strong-motion accelerograms recorded in the lakebed zone were characterized by high amplitudes relative to the lower amplitudes in the epicentral regions and by the extremely long durations (Anderson *et al.*, 1986). The extreme damage during the earthquake occurred as a result of the unusually strong shaking due to the presence of 10–100-m-thick soft clay (e.g., Seed *et al.*, 1988). To investigate the effects of local site amplification and the Mexico City basin (MCB) on the lakebed seismograms, numerous studies have been performed. The study history was summarized in several studies (e.g., Chavez-Garcia and Bard, 1994). There were two important issues.

As an important issue, the large amplitudes of the lakebed accelerograms received much attention (e.g., Seed *et al.*, 1988; Singh *et al.*, 1988). The strong motions were found to be amplified by factors up to 50 in surface layers at the resonant periods of the grounds. Although Seed *et al.* (1988) used a 1D vertical *S*-wave model to interpret the large amplitudes, Sanchez-Sesma *et al.* (1988) and Kawase and Aki (1989) questioned their interpretation, because the observed amplification of the strong motions was too large to be explained by a 1D propagator. Afterward, Shapiro *et al.* (2001) attempted to explain the large amplification produced in surface layers using the eigenfunctions of surface waves without damping. We performed two studies (Iida and Kawase, 2004; Iida, 2007b) described in the Introduction section to explain the large amplification at soft-soil sites.

Table 1
Velocity Model Used at the Roma-C Station

Depth (m)	*P*-Wave Velocity (m/s)	*S*-Wave Velocity (m/s)	Density (g/cm^3)
0–5	1430	90	1.2
5–12	1430	30	1.1
12–25	1430	55	1.1
25–33	1430	80	1.2
33–36	1430	200	1.4
36–44	1430	130	1.4
44–55	1780	400	1.5
55–65	1580	250	1.5
65–102	1750	430	1.7
102–122	1940	660	1.7
122–130	1750	430	1.7
130–138	2250	920	1.9
138–160	1760	500	1.8
160–177	2070	670	1.8
177–200	2500	1120	2.0
200–1000	2600	1120	2.0
> 1000	2600	1120	2.0

The shallow velocity profile above 200 m was measured (Yamashita Architects & Engineers, Inc., and Oyo Corporation, 1990), and the deep structure below 200 m is inferred from four deep *P*-wave profiles (Gutierrez *et al.*, 1994).

Table 2
Velocity Model Used at the Zaragoza Station

Depth (m)	*P*-Wave Velocity (m/s)	*S*-Wave Velocity (m/s)	Density (g/cm^3)
0–5	1420	40	1.1
5–23	1420	28	1.1
23–38	1420	42	1.1
38–40	1420	180	1.2
40–52	1420	76	1.1
52–57	1420	135	1.4
57–67	1700	460	1.4
67–80	1450	140	1.5
80–90	1750	450	1.6
90–1000	2700	1150	2.0
> 1000	2700	1150	2.0

The shallow velocity profile above 90 m was measured, and the deep structure below 90 m is inferred from four deep *P*-wave profiles.

Another important issue was the interpretation of the long duration of the lakebed strong motions. In the late 1980s, studies tried to interpret the long coda waves (e.g., Bard *et al.*, 1988). However, all hypotheses to interpret the long coda waves were disproved with realistic numerical modeling by Chavez-Garcia and Bard (1994), who demonstrated that large attenuation played an important role in the wave propagation in the MCB. It was also revealed that the long coda was present even in a broadband hill seismogram (Singh and Ordaz, 1993).

In the late 1990s, using numerical simulations, it was shown that the low *S*-wave velocity of the Mexican volcanic belt (MVB), which has a broad east–west-trending extent including the Valley of Mexico, played a significant role in increasing the amplitudes and in prolonging the durations of the resonance of the ground motions in the basin (e.g., Shapiro *et al.*, 1997). This hypothesis provided a clue to interpret the long-duration vibration. Recently, *Q* and *Lg* waves in the MVB were investigated (Singh *et al.*, 2007), and the crustal structure below the Valley of Mexico was estimated (Cruz-Atienza *et al.*, 2010). As a recent trend, while 2D or 3D wave-propagation simulations were increasing, few studies were evaluating the vertical amplification of ground motions.

In the present study, we analyze accelerogams recorded at four strong-motion borehole stations located in the three geotechnical zones of Mexico City (Fig. 1). Each borehole station has one surface and two downhole sensors. The seismic sensors of the four stations recorded accelerograms with long coda during the 14 September 1995 M_s 7.3 earthquake, which took place on the Pacific coast in the state of Guerrero. The high-quality accelerograms were utilized in previous studies (e.g., Iida and Kawase, 2004; Iida, 2007b). In the present study, only the accelerograms from the single event are analyzed. Perhaps, because local features are more important than source directivity, we employ the original two horizontal components, not the radial and transverse components.

Shallow (about 100 m) velocity profiles were surveyed at the four borehole stations (Yamashita Architects and Engineers, Inc., and Oyo Corporation, 1990). There are also four deep (about 2500 m) *P*-wave velocity profiles measured in the Valley of Mexico (Gutierrez *et al.*, 1994). By combining the shallow velocity profiles and the deep *P*-wave velocity profiles, an intermediate-depth (1000 m) velocity model is constructed at two soft-soil stations (Tables 1 and 2), and is employed throughout the present study. The reason for employing only two soft-soil stations will be explained in the Vertical Amplitude Ratios section.

The shallow velocity profiles were obtained by suspension *P*–*S* logging. The profiles at the two soft-soil stations are typical of the stratigraphy in the lakebed zone. The unusual *S*-wave velocity and density are caused by unconsolidated, water-saturated clay deposits. In Iida (2007b), employing the combined intermediate-depth velocity model, the theoretical amplitude ratios for various seismic waves between the surface and the depth of the deepest downhole instrument were evaluated and were compared with the observed amplitude ratio at each of the four borehole stations (figs. 6 and 7 of Iida, 2007b). Judging from the results, the adequacy of the combined intermediate-depth velocity model was basically justified.

We make use of the recordings that were obtained at the surface and the deepest downhole instruments at each station. Using the shallow velocity profiles, the theoretical primary and secondary predominant periods of *S* waves and the one-way propagation times of vertically incident direct *S* waves between the surface and the deepest downhole instruments are calculated at the four stations (Table 3). The theoretical predominant periods are calculated by a matrix formulation of elastic wave theory (e.g., Haskell, 1960).

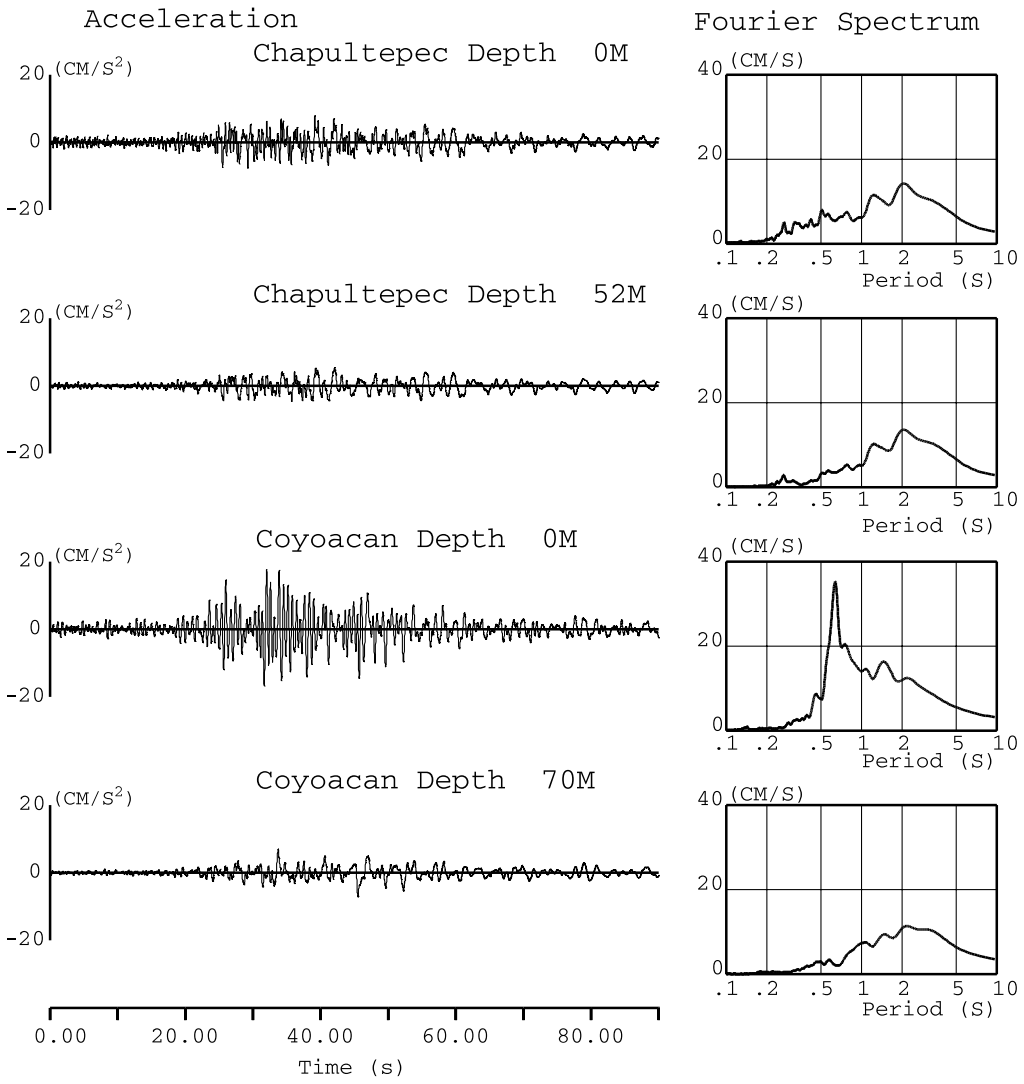

Figure 2. The surface and the downhole accelerograms recorded at the Chapultepec and Coyoacan stations of the 14 September 1995 earthquake. Their Fourier spectra are shown on the right.

As the beginning of the analytical estimations of ground motions, the surface and the deepest downhole accelerograms recorded at two firm-soil stations and at two soft-soil stations are displayed in Figures 2 and 3, respectively. The time axes are not common to the four stations, because synchronization of the recordings is not required in the present study. The surface recordings have a spectral peak around 2.0 s, except for the Coyoacan recording, and indicate inherent predominant periods that depend largely on local features. On the other hand, the downhole recordings commonly show that ~2.0-s ground motions are dominant, because they are less affected by the surface layers.

Vertical Amplitude Ratios

The vertical amplitude ratios between the surface and the deepest downhole recordings are calculated in the following. Also, a nonstationary cross-correlation analysis is performed to identify *S* waves and surface waves. Figure 4

Table 3
Summary of Evaluated Values at the Four Stations

Station	Chapultepec	Coyoacan	Roma-C	Zaragoza
Primary predominant period of *S* waves (s)	0.43	0.70	2.47	4.58
Secondary predominant period of *S* waves (s)	0.18	0.33	1.08	1.74
One-way propagation time of direct *S* waves (s)	(0.13)	(0.20)	0.75	1.45
Longest effective period (s)	(0.53)	(0.80)	3.00	5.81

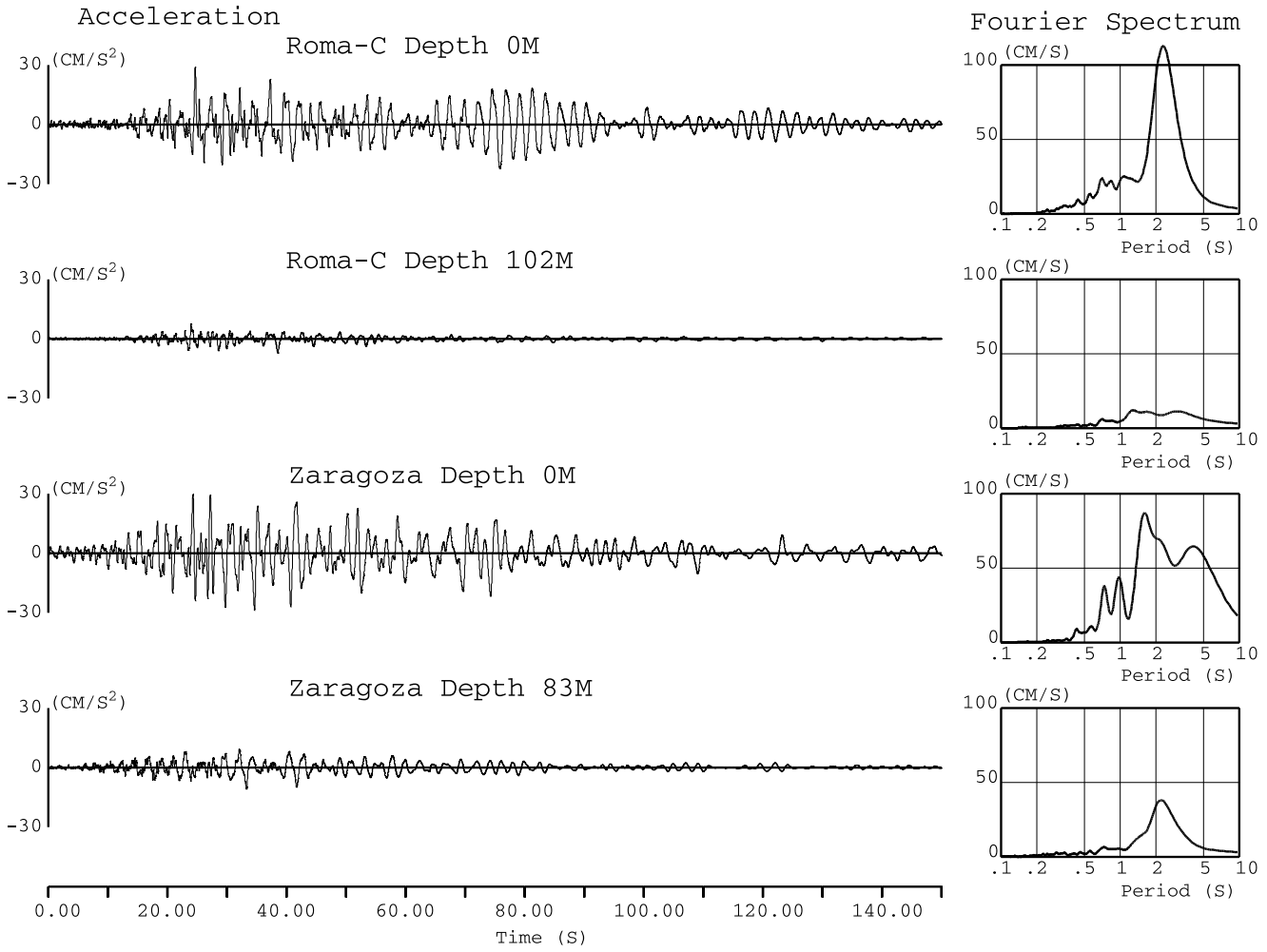

Figure 3. The surface and the downhole accelerograms recorded at the Roma-C and Zaragoza stations. Their Fourier spectra are shown on the right.

shows the amplitude ratios between the surface and the deepest downhole accelerograms recorded at the four borehole stations. They are calculated by taking spectral ratios of signals recorded at two depths of the vertical array. Following Iida and Kawase (2004) and Iida (2007b), the phrase "an amplitude ratio" is used in the present study. A large amplification peak is observed around the theoretical primary predominant period of *S* waves (Table 3) at each station.

Taking into account the surface and downhole accelerograms (Figs. 2 and 3), the amplitude ratios (Fig. 4), and the fundamental resonant periods of buildings (more than 0.5 s), ground motions at the two soft-soil stations located in the lakebed zone are obviously of engineering importance. The large amplitudes of horizontal ground motions observed in the lakebed zone have been pointed out in many studies (e.g., Seed *et al.*, 1988; Chavez-Garcia and Bard, 1994). Therefore, in the following, ground motions are analyzed only at the two soft-soil stations, at which large differences were recognized among the amplitude ratios derived from observation, *S* waves, and Love waves (Iida, 2007b). In contrast, at the two stiff-soil stations, large differences were not recognized among them. These contrasting results indicated the importance of the combined effects of soft soils and the MCB.

Because the accelerograms at the two soft-soil stations have very long duration, the nonstationary observed amplitude ratios are evaluated to reveal the variations. They will be compared with the theoretical amplitude ratios of seismic waves in the Inertial Force and Seismic Waves section. The nonstationary observed amplitude ratios at the Roma-C station and the Zaragoza station are exhibited in Figures 5 and 6, respectively. To gain stable amplitude ratios, a long time window (40 s) is used. In these two figures, the amplitude ratios at the primary predominant periods are significant. Evidently, the nonstationary amplitude ratios are highly variable, and reach an even 100 times at the Roma-C station. On the contrary, variations of the nonstationary amplitude ratios are relatively moderate at the Zaragoza station. The vertical scale differs for the two stations. Soil damping should be constant throughout the long duration because soil behavior is linear for the recording amplitudes.

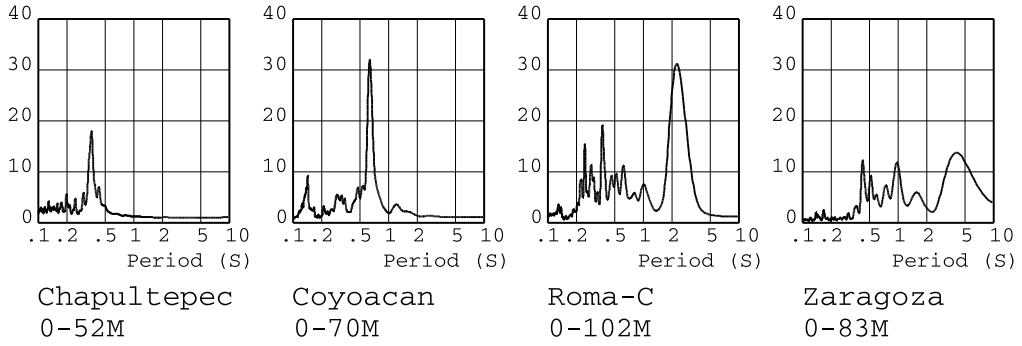

Figure 4. Observed amplitude ratios between the ground surface and the downhole instruments at the four stations.

On the other hand, a nonstationary cross-correlation analysis is conducted between the surface and the deepest downhole recordings to identify *S* waves and surface waves qualitatively. This analysis was successfully performed in several studies (e.g., Iida, 1999, 2007b). In the present study, this analysis is again adopted to confirm that observed ground motions are mainly surface waves around the primary predominant period. The one-way propagation times of direct *S* waves between the surface and downhole instruments are shown in Table 3. If ground motions are *S* waves, a peak of the cross-correlation function should appear at a lag time of the one-way propagation time. For most surface waves, a peak is expected to appear at a lag time of 0.0 s. The peak value falls within a numerical range between −1.0 and 1.0. The longest effective period of a cross-correlation analysis is four times the one-way propagation time and is also listed in Table 3.

Because of the period dependence of observed S and surface waves, band-pass-filtered recordings are cross correlated. The cross-correlation functions in a narrow period band, including the theoretical primary predominant period at the Roma-C station and the Zaragoza station, are plotted in Figures 7 and 8, respectively. The two period bands are wide enough for the frequency resolution determined by the length (15 s) of the time window. A succession of time windows without overlap with their neighbors is used.

At the Roma-C station, there are peaks for *S* waves (at a lag time of 0.75 s) in the cross-correlation functions for some time windows and peaks for surface waves in the functions for other time windows. These functions probably imply that ground motions are a complex mixture of *S* waves and surface waves. At the Zaragoza station, although no clear peaks for *S* waves (1.45 s) exist, peaks for surface waves are identified in the functions for several time windows. Thus, a considerably large ratio of ground motions is found to be surface waves around the primary predominant period at both stations. For reference, the nonstationary cross-correlation functions for shorter-period ground motions at the two stations were exhibited in figure 9 of Iida (2007b). The functions indicated that ground motions were mainly *S* waves in the shorter-period bands.

Inertial Force and Seismic Waves

In the following, the vertical amplitude ratios for inertial force excitation, *S* waves, and surface waves are calculated at the two soft-soil stations. Inertial force excitation is usually used in the engineering community for simplicity. Because most seismologists are unfamiliar with inertial force excitation, the mathematical expressions for the ground motions due to inertial force excitation are given in a standard way in the following paragraphs. As surface waves, the fundamental modes of Love waves and Rayleigh waves are considered. For our intermediate-depth (1000 m) velocity model, the possibilities of first-overtone modes were precluded in Iida (2007b). The vertical amplitude ratios are compared with the observed vertical amplitude ratio. This significant comparison has never been made. Furthermore, the nonstationary observed vertical amplitude ratios are interpreted by means of surface waves.

The ground motions due to inertial force excitation are evaluated using an equation of motion:

$$\mathbf{M}\{\delta^2\chi/\delta t^2\} + \mathbf{C}\{\delta\chi/\delta t\} + \mathbf{K}\{\chi\} = \mathbf{F}, \qquad (1)$$

in which **M** is the mass matrix, **C** is the damping matrix, **K** is the stiffness matrix, χ is the displacement vector, and **F** is the external force vector. As inertial force, a downhole accelerogram is forced toward the shallow velocity model above the downhole instrument. The external force is expressed by

$$\mathbf{F} = -\mathbf{M}\{\delta^2\alpha/\delta t^2\}, \qquad (2)$$

in which α is the external displacement on the bottom boundary of the shallow velocity model. Wave propagation is not considered at all.

The absolute response acceleration on the ground surface is obtained by summing the evaluated relative response acceleration $\delta^2\chi/\delta t^2$ and the input base acceleration $\delta^2\alpha/\delta t^2$. The vertical amplitude ratio is calculated from the obtained surface accelerogram and the original downhole accelerogram. In the present study, spatially constant Rayleigh-type damping of $h = h_1 = h_2$ is employed, in which h_1 and h_2 denote the damping factors evaluated at the primary and sec-

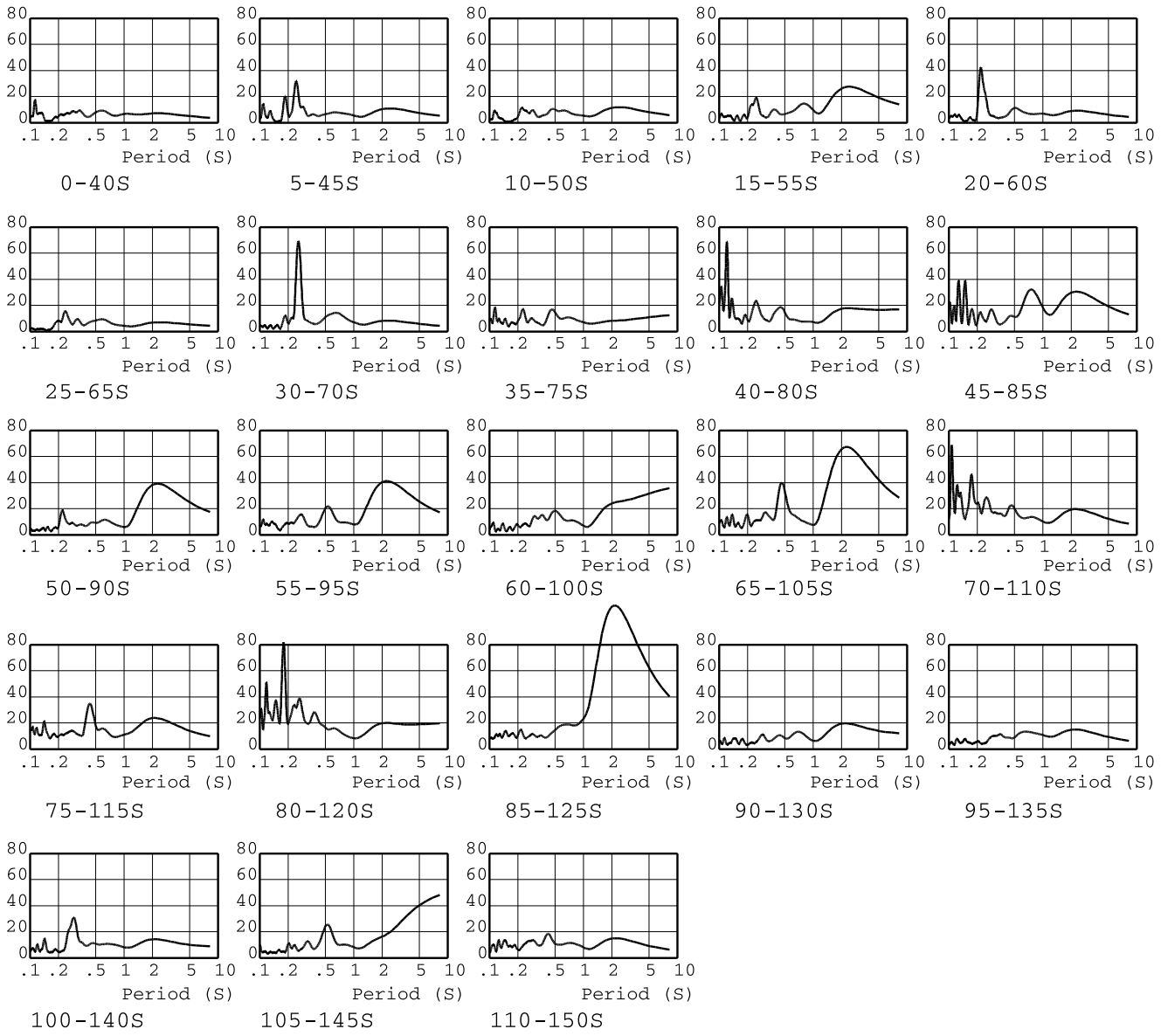

Figure 5. Nonstationary observed amplitude ratios between the ground surface and the 102-m-deep downhole instrument at the Roma-C station. A time window with a length of 40 s is shifted at every 5 s.

ondary natural angular frequencies ω_1 and ω_2 of the shallow velocity model, respectively. In this damping case, the damping matrix is expressed by

$$\mathbf{C} = 2h\omega_1\omega_2/(\omega_1 + \omega_2)\mathbf{M} + 2h/(\omega_1 + \omega_2)\mathbf{K}. \qquad (3)$$

A damping factor of $h = 0.05$, which is equivalent to the quality factor $Q = 10$, is assumed for the entire shallow velocity model. Here, there is an approximate relationship of $h = 1/2Q$. This damping value is presumably underestimated for the very soft lakebed clay.

The mathematical expressions for S waves and surface waves were described fully in Iida (2007b). Regarding S waves, the amplitude ratios are calculated by a matrix formulation (e.g., Haskell, 1960) for the shallow velocity model. In the present study, we employ the same velocity models (Tables 1 and 2) as Iida (2007b), in which the assumed damping value was presumably underestimated for the very soft lakebed clay.

As for surface waves, we follow the mathematical expressions given by Harkrider (1964). Because no damping was considered in his expressions, damping was incorporated into our expressions (Iida, 2007b). In Iida (2007b), to properly estimate the eigenfunctions of surface waves with period-dependent damping, an intermediate-depth (1000 m) velocity model including a complete shallow velocity profile was employed at the two soft-soil stations. In the present study, the same velocity models (Tables 1 and 2) as Iida (2007b) are employed as the standard velocity model. Varied velocity models are also adopted for the purpose of explaining the nonstationary observed vertical amplitude ratios.

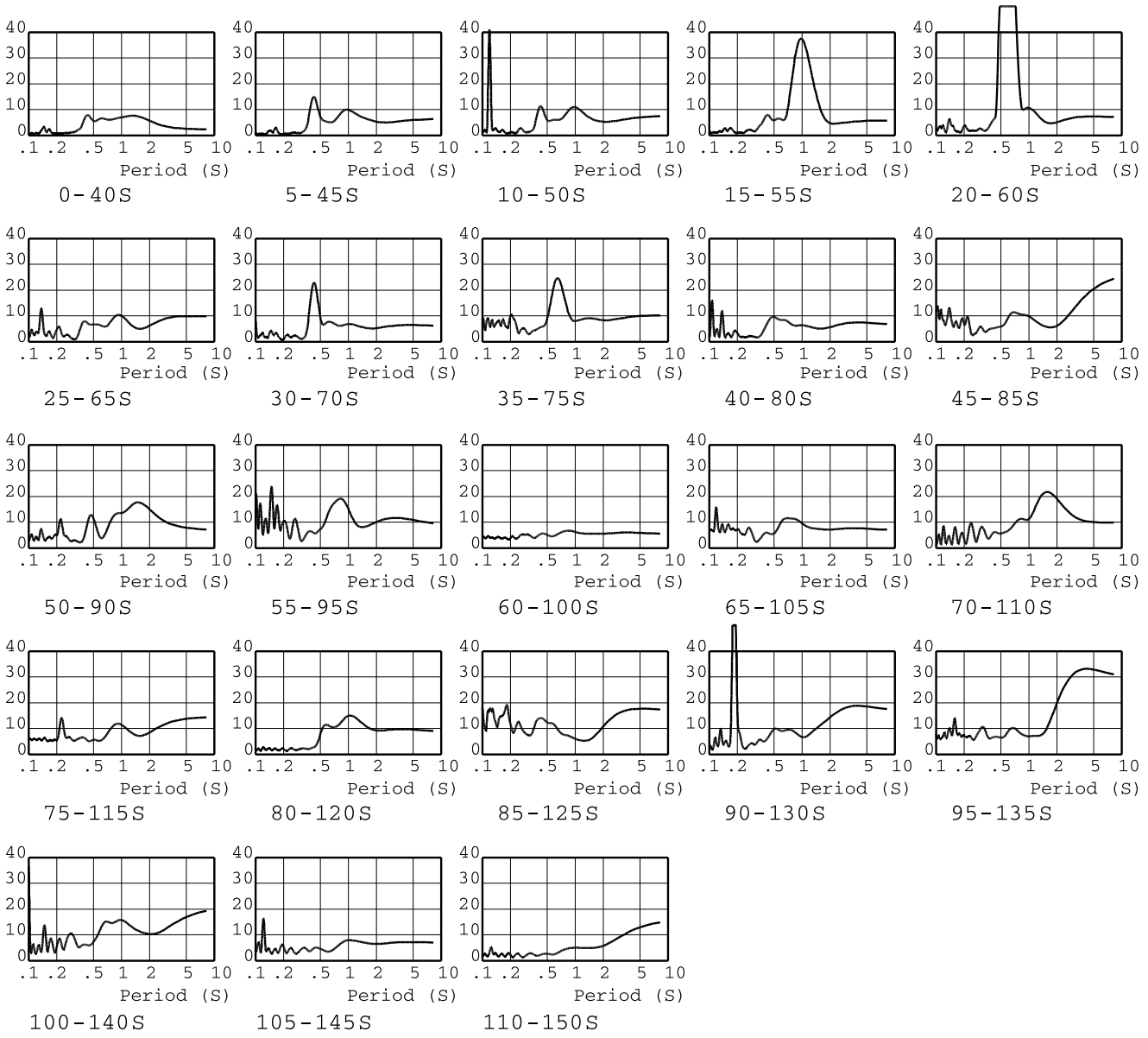

Figure 6. Nonstationary observed amplitude ratios between the ground surface and the 83-m-deep downhole instrument at the Zaragoza station. Note that excessively large peaks are truncated in this figure.

The five types of amplitude ratios obtained at the Roma-C station and the Zaragoza station are displayed in Figures 9 and 10, respectively. First of all, the overall features are similar between both stations, and the predominant period is much the same among the five types of the amplitude ratios at each station. Importantly, the peak amplitude ratios for inertial force excitation and *S* waves around the resonant periods of the grounds are too small to explain the large observed peak amplitude ratios at both stations. The assumed damping value was presumably underestimated for both inertial force excitation and *S* waves. Nevertheless, the ratios are too small.

The amplitude ratios for Love waves and Rayleigh waves are essential. Love waves are able to reproduce the large observed peak amplitude ratios sufficiently at both stations. As will be shown in the following, the amplitude ratios for surface waves can be controlled by not only the damping for the eigenfunctions of surface waves but also the depth of the structure in which surface waves are trapped. In contrast, although the interpretation as Rayleigh waves for the observed amplitude ratios is plausible at the Roma-C station, the interpretation is not appropriate at the Zaragoza station.

To explain the nonstationary observed amplitude ratios further, the amplitude ratios for surface waves are evaluated using varied velocity models. At the Roma-C station, a shallow velocity model and an alternative velocity model equivalent to a deep velocity model were tested. As a shallow velocity model, a 200-m-deep velocity model was adopted. On the other hand, a deep velocity model was not available because the solutions could not be obtained owing to the large contrasts in the material properties between the shallow

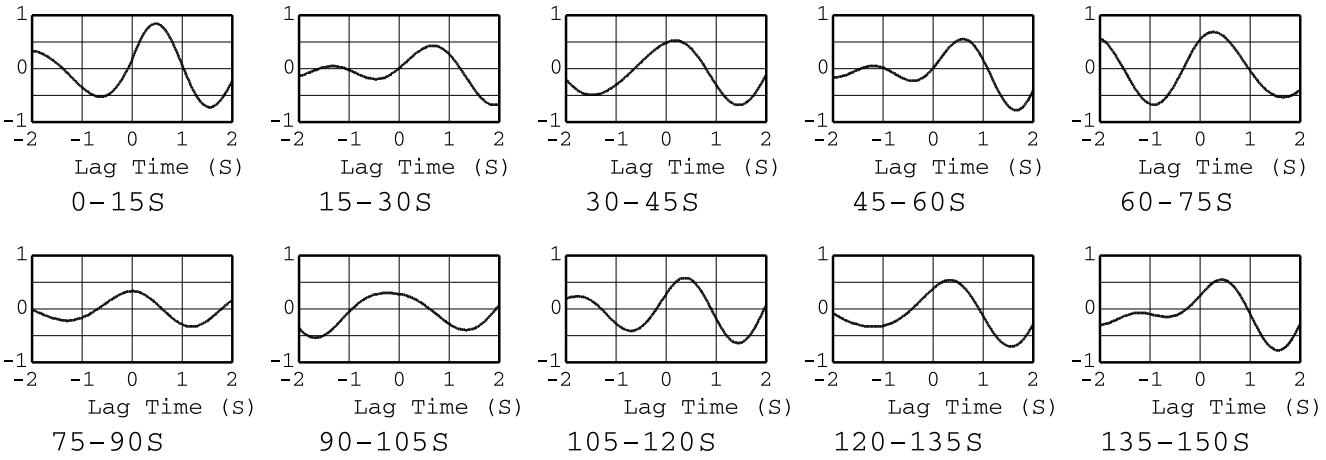

Figure 7. Nonstationary cross-correlation functions for a 2.0–3.0-s period band including the primary predominant period (2.5 s) between the surface and the downhole (102 m) accelerograms recorded at the Roma-C station. A time window with a length of 15 s is shifted without overlap.

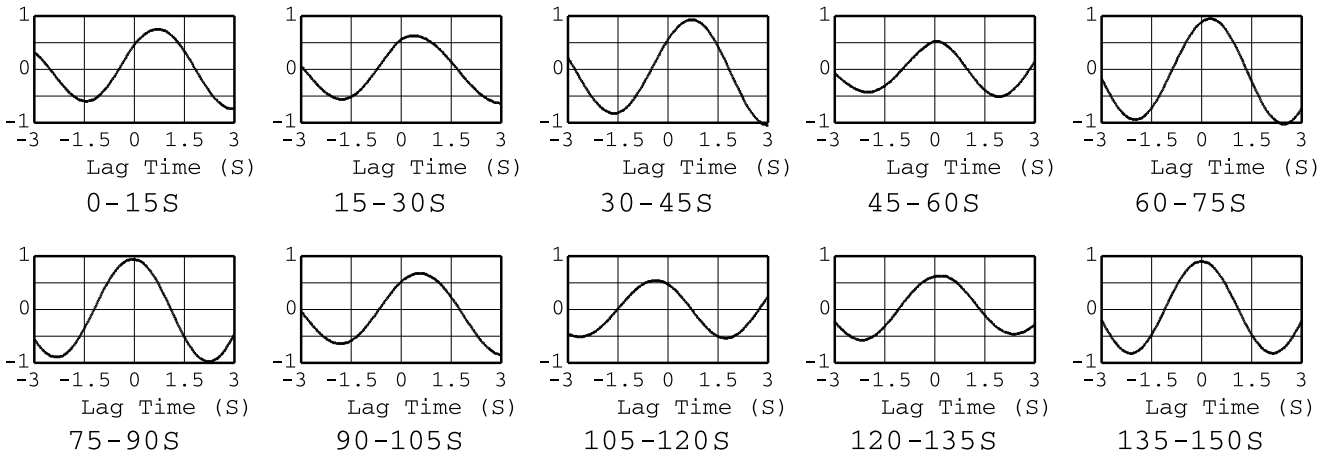

Figure 8. Nonstationary cross-correlation functions for a 4.0–6.0-s period band including the primary predominant period (4.6 s) between the surface and the downhole (83 m) accelerograms recorded at the Zaragoza station.

portion and the deep portion. In place of a deep velocity model, a 5/3 times larger damping (3/5 times smaller Q) velocity model than the standard velocity model was adopted. The alternative velocity model should be roughly comparable in terms of dissipation of the confined energy.

The amplitude ratios for surface waves calculated using two additional velocity models are displayed in Figure 11. It is found that the amplitude ratios for Love waves are greatly controlled by the depths of the structures in which Love waves are trapped and are able to provide a good explanation for the nonstationary observed amplitude ratios. As the depth of the structure becomes shallower, the amplitude ratio gets larger. In contrast, Rayleigh waves are not suitable for explaining the nonstationary observed amplitude ratios because the solutions are unstable.

At the Zaragoza station, neither a deep velocity model nor a larger damping velocity model worked well. The solutions could not be obtained. Hence, two shallow velocity models were tested, and the amplitude ratios for surface waves are shown in Figure 12. The amplitude ratios for Love waves are quite inadequate for explaining the nonstationary observed amplitude ratios, because the predominant period changes significantly with the depth of the structure in which Love waves are trapped. A sufficiently deep (about 1000 m) structure is required for producing the observed amplitude ratios at the predominant period. It is obvious that Rayleigh waves are not a good candidate to account for the nonstationary observed amplitude ratios. Rather, this figure gives an indication that the two shallow velocity models excite observed higher-mode surface waves.

Discussion and Conclusions

At the Roma-C station, the nonstationary observed amplitude ratios were highly variable. The large variations could be explained well by mixture of S waves and Love waves. Moreover, they could be explained better by addition of the depths of the structures in which Love waves are trapped.

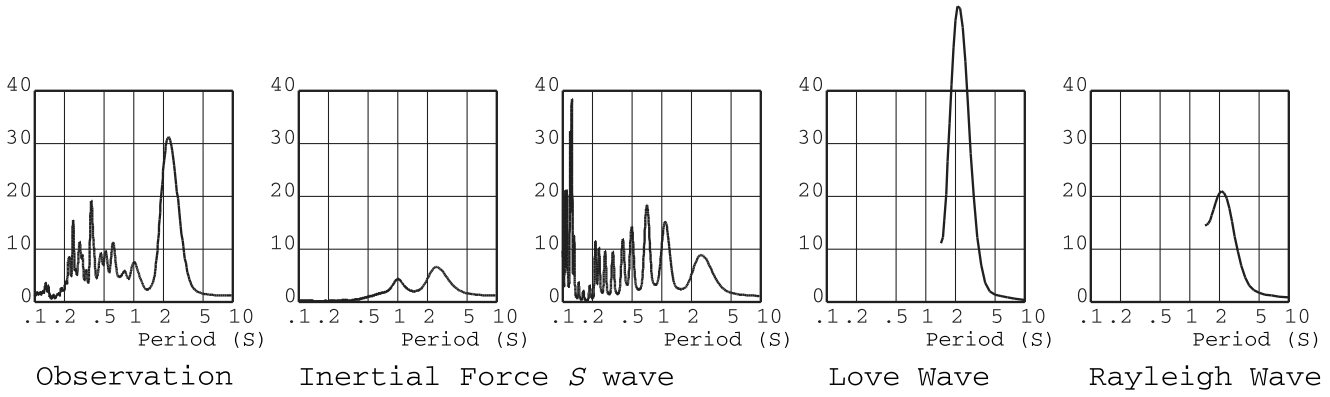

Figure 9. Comparison of amplitude ratios between the ground surface and the 102-m-deep downhole instrument at the Roma-C station. The amplitude ratios are derived from observation, inertial force excitation, *S* waves, Love waves, and Rayleigh waves.

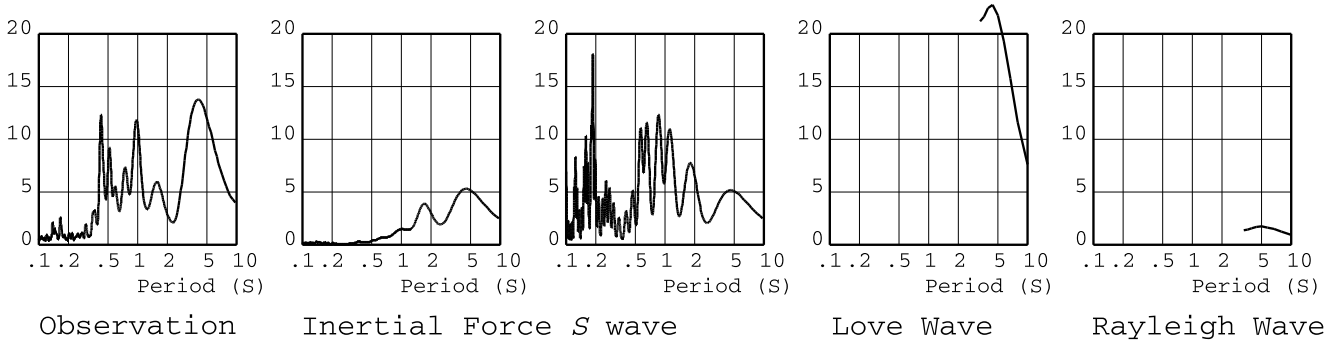

Figure 10. Comparison of amplitude ratios between the ground surface and the 83-m-deep downhole instrument at the Zaragoza station. The amplitude ratios are derived from observation, inertial force excitation, *S* waves, Love waves, and Rayleigh waves.

The structures correspond to the MCB. The MCB model used in wave-propagation simulations for the MVB and the MCB conducted in Iida and Kawase (2004) is a good example. The Roma-C station is located in the marginal area of the MCB (Fig. 1). Therefore, Love waves seem to be trapped in several structures with depths such as 200 and 1000 m.

As for the Zaragoza station, in contrast, the nonstationary observed amplitude ratios remained comparatively stable. The stable amplitude ratios could be interpreted basically by the mixture of *S* waves and Love waves. Also, the depth of the structure in which Love waves are trapped was about 1000 m. The structure corresponds to the MCB. The Zaragoza station is located in the central area of the MCB (Fig. 1). Therefore, it is believed that the wavefield is not changed very much throughout the long duration.

From the viewpoints of engineering applications, inertial force excitation seemed to reproduce theoretical amplification of *S* waves relatively well (Figs. 9 and 10). However, it was evidently unable to retrieve the eigenfunctions of Love waves. The retrieval of the eigenfunctions of Rayleigh waves was not possible as well. Therefore, instead of inertial force excitation, the theoretical amplitude ratios of seismic waves should be employed.

In the engineering community, the maximum vertical amplification of ground motions is very important. Because the amplitude ratio of Love waves was found to be the primarily significant factor, the depth of the structure in which Love waves are trapped is of practical importance at a soft-soil site in a deep basin. Here, we need to remember that, as the depth of the structure becomes shallower, the amplitude ratio gets larger. Hence, a rather deep basin structure including a complete shallow velocity profile with likely damping must be well characterized. Thus, the possible maximum surface ground motions can be estimated approximately from subsurface ground motions as base motions, which have less local variations.

The lakebed clay layers in Mexico City are composed of some the softest soils in the world. Hence, the characterization of seismic waves at the two soft-soil stations was extraordinarily difficult. Although the characterization was not perfect, it was considered to be sufficient. Therefore, the same characterization should be feasible in almost all geotechnical environments. Moreover, in not a few geotechnical areas, owing to strong nonlinear behavior of soils or soil liquefaction, the original rigidity of the surface layers might be largely decreased to lower rigidity, such as the lakebed clay layers. Therefore, the five types of amplitude ratios evaluated in the present study are greatly significant.

At the two soft-soil stations in Mexico City, while the large time variations in the vertical amplification of ground motions were interpreted, inertial force excitation was inter-

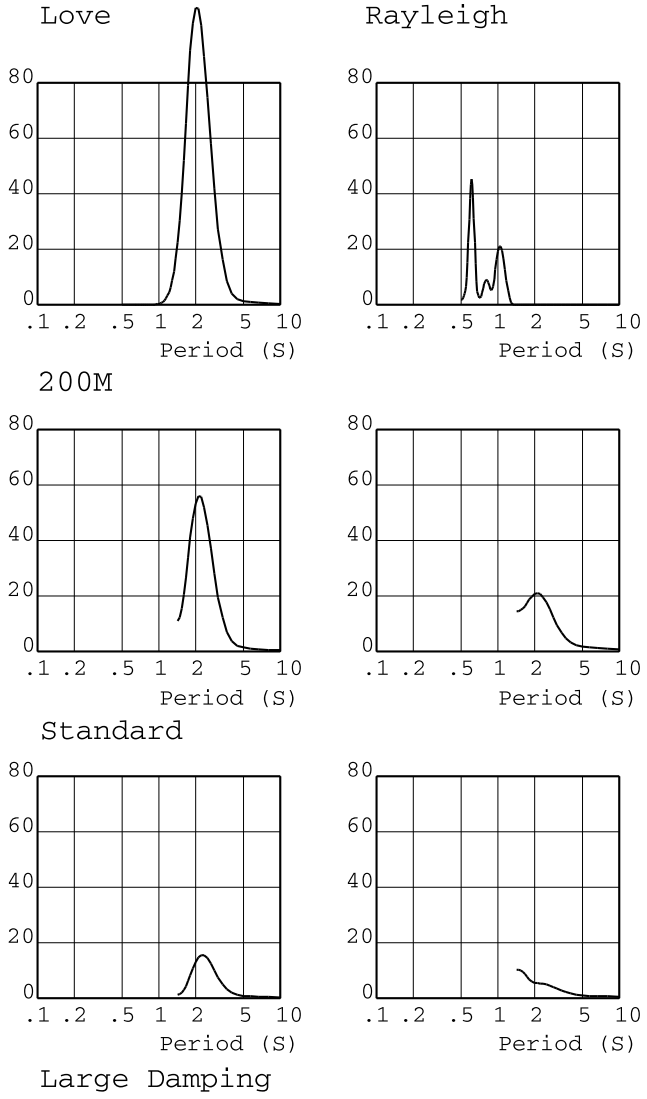

Figure 11. Various amplitude ratios for Love waves and Rayleigh waves between the ground surface and the 102-m-deep downhole instrument at the Roma-C station. The amplitude ratios are obtained using a 200-m-deep velocity model, standard (1000-m-deep) velocity model, and large damping velocity model.

preted in terms of seismic waves. The conclusions are as follows: (1) the large time variations in the vertical amplification of ground motions can be explained sufficiently by both the mixture of *S* waves and Love waves and the depth of the structure in which Love waves are trapped, a structure corresponding to the MCB; (2) although inertial force excitation is considered to be valid for *S* waves, it proves to be invalid for Love waves. As an additional remark, because a single earthquake was analyzed in the present study, the uncertainties need to be recognized.

Data and Resources

The strong-motion accelerograms are open to researchers and were provided by the National Disaster Prevention Center of Mexico.

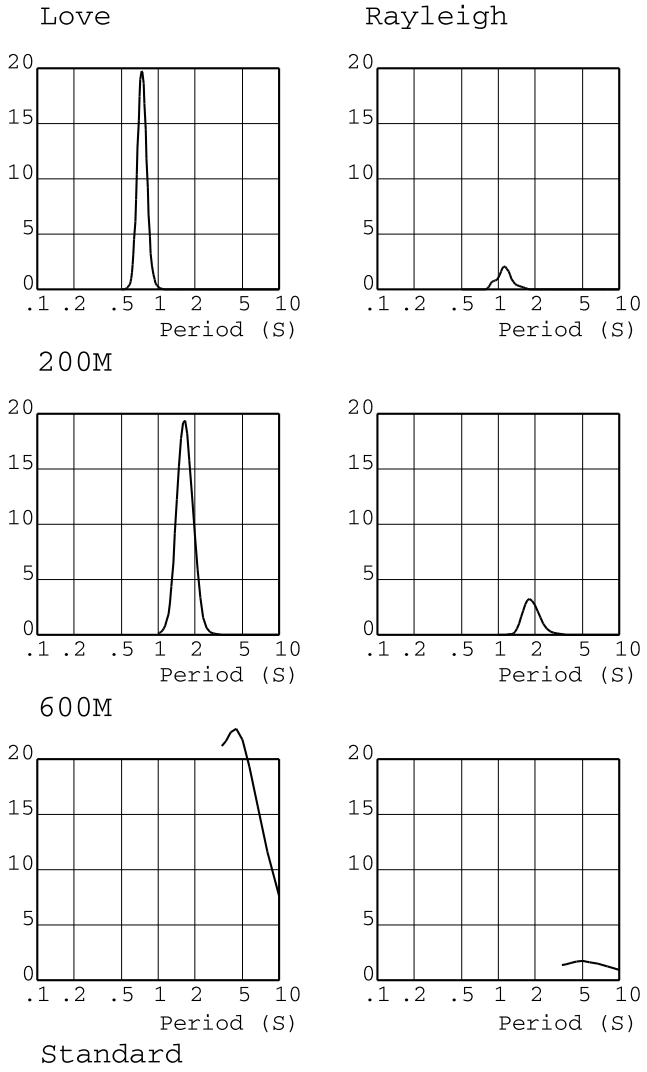

Figure 12. Various amplitude ratios for Love waves and Rayleigh waves between the ground surface and the 83-m-deep downhole instrument at the Zaragoza station. The amplitude ratios are obtained using a 200-m-deep velocity model, 600-m-deep velocity model, and standard (1000-m-deep) velocity model.

Acknowledgments

Roberto Quaas and Carlos Gutierrez of the National Disaster Prevention Center of Mexico supplied the strong-motion accelerograms and the deep *P*-wave profiles, respectively. The critical reviews by Associate Editor Ivan Wong and two anonymous reviewers greatly improved the article.

References

Anderson, J. G., P. Bodin, J. N. Brune, J. Prince, S. K. Singh, R. Quaas, and M. Onate (1986). Strong ground motion from the Michoacan, Mexico earthquake, *Science* **233,** 1043–1049.

Bard, P.-Y., M. Campillo, F. J. Chavez-Garcia, and F. Sanchez-Sesma (1988). The Mexico earthquake of September 19, 1985. A theoretical investigation of large- and small-scale amplification effects in the Mexico City valley, *Earthq. Spectra* **4,** 609–633.

Chavez-Garcia, F. J., and P.-Y. Bard (1994). Site effects in Mexico City eight years after the September 1985 Michoacan earthquakes, *Soil Dynam. Earthq. Eng.* **13,** 229–247.

Cruz-Atienza, V. M., A. Iglesias, J. F. Pacheco, N. M. Shapiro, and S. K. Singh (2010). Crustal structure below the Valley of Mexico estimated from receiver functions, *Bull. Seismol. Soc. Am.* **100,** 3304–3311.

Gutierrez, C. A., K. Kudo, E. Nava, M. Yanagizawa, S. K. Singh, F. J. Hernandez, and K. Irikura (1994). Refraction profile in the south of Mexico City and the correlation with other information sources, *Geological Hazard/01/94*, National Disaster Prevention Center, Mexico City (in Spanish).

Harkrider, D. G. (1964). Surface waves in multilayered elastic media. I. Rayleigh and Love waves from buried sources in multilayered elastic halfspace, *Bull. Seismol. Soc. Am.* **54,** 627–679.

Haskell, N. A. (1960). Crustal reflection of plane *SH* waves, *J. Geophys. Res.* **65,** 4147–4150.

Iida, M. (1999). Excitation of high-frequency surface waves with long duration in the Valley of Mexico, *J. Geophys. Res.* **104,** no. B4, 7329–7345.

Iida, M. (2000). A systematic method for analyzing borehole recordings to estimate the wavefield in the lakebed zone of Mexico City, *Bull. Seismol. Soc. Am.* **90,** 1268–1280.

Iida, M. (2006). Three-dimensional linear and simplified nonlinear soil response methods based on an input seismic wave field, *Int. J. Geomech.* **6,** 342–355.

Iida, M. (2007a). Estimation of the wave fields in the three geotechnical zones of Tokyo, *Bull. Seismol. Soc. Am.* **97,** 575–590.

Iida, M. (2007b). Excitation of surface waves in the Valley of Mexico, *Bull. Seismol. Soc. Am.* **97,** 1458–1474.

Iida, M. (2013). Three-dimensional finite-element method for soil–building interaction based on an input wave field, *Int. J. Geomech.* **13,** 430–440.

Iida, M., and H. Kawase (2004). A comprehensive interpretation of strong motions in the Mexican volcanic belt, *Bull. Seismol. Soc. Am.* **94,** 598–618.

Iida, M., M. Iiba, K. Kusunoki, Y. Miyamoto, and H. Isoda (2015). Seismic responses of two RC buildings and one wood building based on an input wave field, *Int. J. Geomech.* **15,** 04014093.

Iida, M., H. Yamanaka, and N. Yamada (2005). Wave field estimated by borehole recordings in the reclaimed zone of Tokyo Bay, *Bull. Seismol. Soc. Am.* **95,** 1101–1119.

Johnson, L. R., and W. Silva (1981). The effects of unconsolidated sediments upon the ground motion during local earthquakes, *Bull. Seismol. Soc. Am.* **71,** 127–142.

Kawase, H., and K. Aki (1989). A study on the response of a soft basin for incident *S*, *P*, and Rayleigh waves with special references to the long duration observed in Mexico City, *Bull. Seismol. Soc. Am.* **79,** 1361–1382.

Kinoshita, S. (1981). A statistical method for estimation of wave transfer function, *Proc. Japan Soc. Civil Eng.* **313,** 1–11 (in Japanese).

Kinoshita, S. (1999). A stochastic method for investigating site effects by means of a borehole array. *SH* and Love waves, *Bull. Seismol. Soc. Am.* **89,** 484–500.

Kinoshita, S., H. Fujiwara, T. Mikoshiba, and T. Hoshino (1992). Secondary Love waves observed by a strong-motion array in the Tokyo lowlands, Japan, *J. Phys. Earth* **40,** 99–116.

Meli, R., and J. A. Avila (1989). The Mexico earthquake of September 19, 1985. Analysis of building response, *Earthq. Spectra* **5,** 1–17.

Sanchez-Sesma, F., S. Chavez-Perez, M. Suarez, M. A. Bravo, and L. E. Perez-Rocha (1988). The Mexico earthquake of September 19, 1985. On the seismic response of the Valley of Mexico, *Earthq. Spectra* **4,** 569–589.

Seed, H. B., M. P. Romo, J. I. Sun, A. Jaime, and J. Lysmer (1988). Relationship between soil conditions and earthquake ground motions, *Earthq. Spectra* **4,** 687–729.

Shapiro, N. M., M. Campillo, A. Paul, S. K. Singh, D. Jongmans, and F. J. Sanchez-Sesma (1997). Surface-wave propagation across the Mexican volcanic belt and the origin of the long-period seismic-wave amplification in the Valley of Mexico, *Geophys. J. Int.* **128,** 151–166.

Shapiro, N. M., S. K. Singh, D. Almora, and M. Ayala (2001). Evidence of dominance of higher-mode surface waves in the lakebed zone of the Valley of Mexico, *Geophys. J. Int.* **147,** 517–527.

Singh, S. K., and M. Ordaz (1993). On the origin of long coda observed in the lake-bed strong-motion records of Mexico City, *Bull. Seismol. Soc. Am.* **83,** 1298–1306.

Singh, S. K., A. Iglesias, D. Garcia, J. F. Pacheco, and M. Ordaz (2007). *Q* and *Lg* waves in the central Mexican volcanic belt, *Bull. Seismol. Soc. Am.* **97,** 1259–1266.

Singh, S. K., J. Lermo, T. Dominguez, M. Ordaz, J. M. Espinosa, E. Mena, and R. Quaas (1988). The Mexico earthquake of September 19, 1985: A study of amplification of seismic waves in the Valley of Mexico with respect to a hill zone site, *Earthq. Spectra* **4,** 653–673.

Yamashita Architects & Engineers Inc., and Oyo Corporation (1990). *Subsurface Investigation Project of the National Disaster Prevention Center, Mexico City* (in Spanish).

Earthquake Research Institute
University of Tokyo
1-1-1, Yayoi, Bunkyo-ku
Tokyo 113-0032, Japan
iida@eri.u-tokyo.ac.jp

Manuscript received 1 November 2015;
Published Online 25 October 2016